How Credible is Hong Kong's Currency Peg?

Urban J. Jermann, Bin Wei, and Vivian Z. Yue*

February 12, 2025

Abstract

In this paper, we develop an asset-pricing model for the Hong Kong dollar (HKD) exchange rate. The model assumes that the HKD-USD peg is not fully credible, and financial markets assign a nonzero probability to its breakdown. We derive an analytical formula for model-implied option prices and use HKD options to estimate the model. Our estimation results suggest that financial markets perceive an increased risk of the peg breaking, driven by recent U.S. interest rate hikes and Hong Kong's slowing economy.

Keywords: Hong Kong dollar, HKD, currency board, peg, central parity

The views expressed in this paper are those of the authors and do not necessarily represent those of the Federal Reserve System. The latest estimation results are available at https://sites.google.com/site/binweiresearch/hkd.

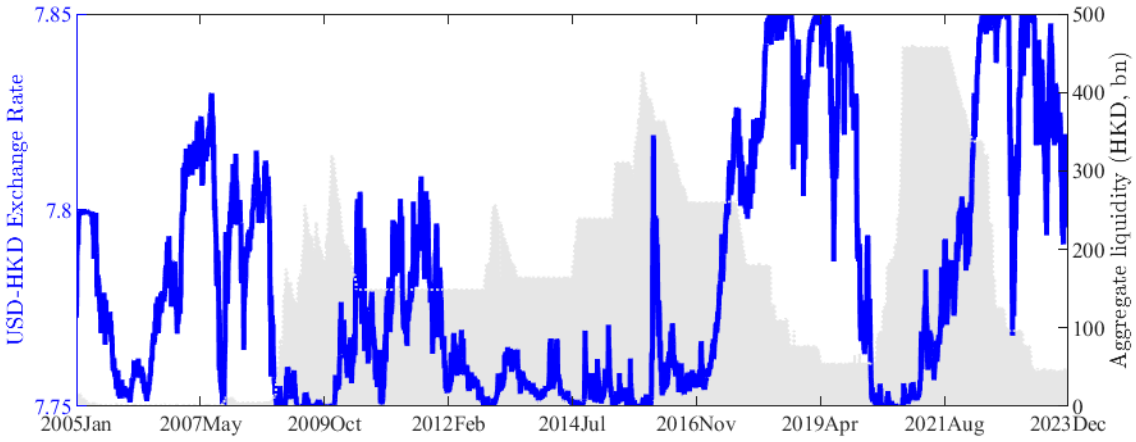
*Jermann is at the Wharton School of University of Pennsylvania and NBER, E-mail: jermann@ wharton.upenn.edu. Wei is at the Federal Reserve Bank of Atlanta, E-mail: bin.wei@atl.frb.org. Yue is at Emory University, NBER, and CEPR, E-mail: vyue@emory.edu.

> "Confidence in the LERS has been tested countless times through difficult events ... The LERS sailed through them all. [W]e have no intention and we see no need to change the LERS."
>
> — *Eddie Yue, HKMA Chief Executive*[1]

1 Introduction

The Hong Kong Dollar (HKD) has been pegged to the U.S. Dollar (USD) at 7.8 HKD per USD since 1983. Under the current currency board arrangement—known as the *Linked Exchange Rate System* or "LERS"—the Hong Kong Monetary Authority (HKMA) has a mandate to keep the spot exchange rate between 7.75 to 7.85 HKD per USD, according to a band set in 2005. This arrangement has long been considered a guarantee of financial stability and economic prosperity in Hong Kong. Figure 1 plots the historical USD-HKD exchange rate since 2005.

Figure 1: **USD-HKD Exchange Rate and Aggregate Liquidity**



NOTE: This figure plots the USD-HKD exchange rate (solid line, left axis) and aggregate banking liquidity in Hong Kong in billion HKD (shaded area, right axis) between January 2005 and December 2023.

When the HKD reaches either end of the band, the authority has intervened to defend the

[1]See Eddie Yue's remarks in "The Linked Exchange Rate System – 40 Years On" on October 17, 2023, at URL: https://www.hkma.gov.hk/eng/news-and-media/insight/2023/10/20231017/.

peg, through buying or selling HKD in the foreign exchange market. For instance, by selling US dollars to buy Hong Kong dollars, the HKMA withdraws cash from the banking system, reducing its aggregate balance and causing interest rates to rise, which would strengthen the Hong Kong dollar and keeps it within the band. If a currency board depletes its foreign reserves, loses its credibility, or faces severe economic shocks, maintaining the fixed exchange rate becomes unsustainable.[2]

Recently, Hong Kong's currency peg has been under increasing pressure. As shown in Figure 1, the Hong Kong dollar has traded on the weak-side of the trading band for much of the time since the U.S. started to raise interest rates in early 2022. As a result, the HKMA had to intervene by buying a large amount of Hong Kong dollars to maintain the peg. Consequently, the aggregate balance or liquidity in the Hong Kong banking system, depicted by the grey shaded area in Figure 1, has declined by more than 90% from its peak in 2021.

An important question thus arises: Is Hong Kong's currency peg still credible? As quoted above, Eddie Yue, chief executive of the HKMA, reiterated the institution's steadfast commitment to the LERS in his speech on October 17, 2023. As another example, he said in May 2023 that local banks have sufficient liquidity to manage with.[3] Not all market participants share this view. For example, some hedge funds, such as Pershing Square Capital Management, have reportedly taken large positions against the HKD. Bill Ackman, the owner of Pershing Square Capital Management, tweeted in November 2023 that "it is a matter of time" before the peg breaks.

In this paper, we develop an asset pricing model of the HKD and measure financial markets' views about the likelihood that the peg would be abandoned based on derivatives data. In the model, the HKD-USD peg is not perfectly credible. The peg will persist into the next period with probability p and will break with a probability $1-p$. If the peg continues, the HKD-USD exchange rate is determined by a no-arbitrage equilibrium condition. If the peg breaks, the exchange rate equals its fundamental value, reflecting the levels that would prevail under a free-floating regime, V.

Under a continuous-time formulation, we show that the equilibrium exchange rate can be expressed as a function of the fundamental value in closed form (Proposition 1). The function is non-linear and S-shaped. This is reminiscent of the so-called "honeymoon effect" in the target-zone literature (see Krugman, 1991) that represents the expectation of potential

[2]For example, Argentina's quasi-currency board collapsed in 2002 due to its failure to maintain full foreign reserves and large persistent trade deficits (Na et al., 2018). Under speculative attacks, Estonia's currency board nearly failed during the Russian financial crisis in 1998.

[3]See Eddie Yue's remarks in "On the operation of the Linked Exchange Rate System" on May 3, 2023, at URL: https://www.hkma.gov.hk/eng/news-and-media/insight/2023/05/20230503.

interventions even when the exchange rate lies inside the zone.

We also derive an analytical formula for option prices implied by the model (Proposition 3). Due to the possibility of a regime shift in the exchange rate system, the option pricing formula differs significantly from the standard Black-Scholes formula. Specifically, our model implies a U-shaped distribution for the HKD-USD exchange rate, closely matching the empirical distribution observed in the data—a stark contrast to the bell-shaped distribution under standard Black-Scholes models.

We estimate the model using HKD options data to assess the probability of the peg breaking as perceived by financial markets. In line with the sharp decline in aggregate liquidity depicted in Figure 1, the estimated probability of the peg breaking surged to approximately 50% in the last quarter of 2022. This elevated likelihood, as viewed by financial markets, had not been seen since the global financial crisis. Concurrently, throughout 2022, the HKD-USD exchange rate consistently hovered at the cheap end of the trading band, indicating substantial depreciation pressure.

Our analysis reveals that higher Hong Kong interest rates strengthen both the fundamental value of the HKD (V) and the peg continuation probability (p), reinforcing confidence in the LERS. Conversely, rising U.S. interest rates has the opposite effect. Liquidity in the banking system supports peg credibility by increasing p, but its decline weakens V, reflecting capital outflows that put stress on the currency board system. Lastly, China's onshore and offshore exchange rates, CNY and CNH, play a crucial role. A stronger yuan supports the HKD's fundamental value, while depreciation in the Chinese currency raises concerns over the peg's sustainability. These findings underscore that the HKD peg's credibility hinges not only on local monetary conditions but also on external pressures from U.S. rate hikes and China's financial stability.

This paper is related to the literature on exchange rate target zones. The canonical target zone model presented in Krugman (1991) has been extended in various ways.[4] All these traditional target zone models rely on the assumption of uncovered interest parity (UIP), which does not hold in the data (see, e.g., Engel, 1996; Lustig et al., 2011). In contrast, we relax UIP and derive the exchange rate through a no-arbitrage condition following Jermann (2017) which uses this approach to estimate the implied survival probability of the Swiss franc cap in 2015. We extend the framework in Jermann (2017) to a continuous-time setting and derive both the equilibrium exchange rate and option prices in closed form. This has the

[4]For example, Bertola and Svensson (1993) incorporates time-varying realignment risk; Froot and Obstfeld (1991a,b) and Delgado and Dumas (1991) introduce intra-marginal mean-reverting interventions; Svensson (1991a,b) derives and tests implications for the term structure of interest rate differentials. Lindberg and Söderlind (1994) contains a structural estimation on Swedish data of an extended target zone model that incorporates both intra-marginal interventions and time-varying realignment risk.

added benefit of making the estimation of the model much more efficient.[5] The analytical option pricing formula derived in our framework with imperfect credibility contributes to the literature on option pricing in a target zone (e.g. Ball and Roma, 1993; Dumas et al., 1995; Hertrich and Zimmermann, 2017).

Our paper is closely related to Genberg and Hui (2011).[6] They extract the risk-neutral probability density function of exchange rate expectations from option prices based on Malz (1997) and study how market expectations respond to reforms of the LERS in September 1998 and May 2005. The methodology in Malz (1997), which is based on the standard Black-Scholes model, usually leads to a bell-shaped probability density function. In contrast, the exchange rate distribution in a target zone like Hong Kong's is U-shaped, indicating that the probability of the exchange rate being near the boundaries is significantly higher than the likelihood of it being near the midpoint of the band. In our paper, we introduce a probability of regime shifts and derive option prices in closed form for target-zone economies. Not only does our model reproduce the U-shaped exchange rate distribution, but it also leads to a more realistic estimate of the probability of the exchange rate breaking out of the band. Moreover, our options-based framework differentiates itself from studies employing regime-switching DSGE or econometric models to assess currency board credibility (e.g., Jeanne and Masson, 2000; Blagov and Funke, 2019; Feng et al., 2023).

In other related work, Hanke et al. (2018) examines how probabilities from betting markets can be combined with risk-neutral exchange rate densities derived from currency options to forecast exchange rate movements around major political events. Our paper complements broader discussions on currency boards and their credibility, as reviewed in Ghosh et al. (2020).

The rest of the paper is organized as follows. In Section 2, we provide a brief overview of Hong Kong's linked exchange rate system. In Section 3, we present our model for the Hong Kong dollar. In Section 4, we report estimation results and discuss key implications. Section 5 concludes.

2 Hong Kong's Linked Exchange Rate System: An Overview

The monetary institution in Hong Kong has evolved from the silver standard (1863–Nov 1935) and the Sterling standard (Dec 1935–Jun 1972), to a brief fixed exchange rate regime

[5] Other papers studying on Swiss franc are Amador et al. (2019); Mirkov et al. (2019); Auer et al. (2021); Breedon et al. (2023).

[6] For other studies on the Hong Kong dollar, see, for example, Kwan and Lui (1999) and Latter (2007).

against the US dollar (Jul 1972–Nov 1974), then to a free-floating regime (Nov 1974–Oct 1983), and finally to the current currency board with a US dollar link (Oct 1983–present).[7]

The current currency board arrangement is implemented through the Linked Exchange Rate System (LERS), introduced on October 17, 1983. Under the LERS, the Hong Kong dollar monetary base is fully backed by US dollar assets held in the Exchange Fund at the fixed exchange rate of HK$ 7.80 to one US dollar (and all changes in the monetary base are also fully matched by corresponding changes in US dollar assets).

The monetary base in Hong Kong comprises the following components: *(i)* Certificates of Indebtedness (CIs), which provide full backing to the banknotes issued by note-issuing banks; *(ii)* Government-issued notes and coins in circulation; *(iii)* Aggregate Balance, which is the sum of clearing account balances kept with the HKMA; and *(iv)* Exchange Fund Bills and Notes issued by the HKMA on behalf of the government for the account of the Exchange Fund.[8]

The government, through the HKMA, has given authorization to three commercial banks to issue banknotes in Hong Kong.[9] Holding CIs give the note issuing banks the right to issue HKD bills with a fixed exchange rate between a CI and the USD at the rate of 7.8 HKD/USD. The fixed value of the CI thus effectively translates into a fixed exchange rate between the HKD and the USD.

With the implementation of real-time gross settlement on December 9, 1996, all banks became obliged to maintain settlement accounts directly with the Exchange Fund. The combined total of clearing balances is known as the Aggregate Balance, which enables the authorities to control the volume of funds in the system directly through open market operations.

Following the Asian Financial Crisis in 1997, the HKMA announced a package of measures, known as the "Seven Technical Measures", on September 5, 1998 to strengthen the mechanism. Two major planks of the technical measures are the provision of a weak-side Convertibility Undertaking (CU) in respect of the Aggregate Balance and modifications to the Discount Window facility. At the rate of HK$ 7.5 per US dollar, the HKMA was committed to purchasing unlimited amounts of HKDs for USDs to prevent the currency from weakening beyond that rate. The weak-side CU was gradually moved from 7.75 to 7.8

[7] See, e.g., Greenwood (2007) and Latter (2007) for a more detailed description of the evolution of the monetary system in Hong Kong.

[8] To facilitate the development of Hong Kong's debt markets, the Exchange Fund Bills program was created in March 1990, and Notes were introduced in March 1993. The Exchange Fund Bills and Notes market enables the authorities to conduct open market operations.

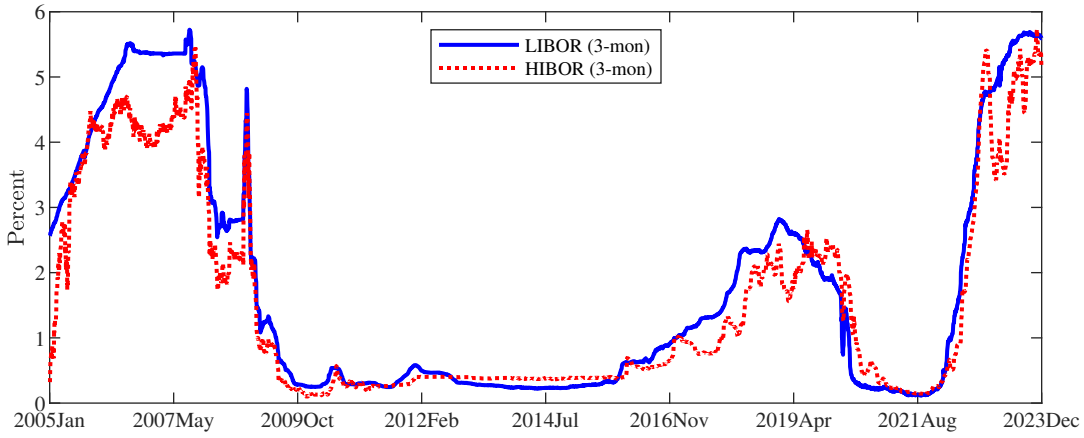
[9] Namely, the Hongkong and Shanghai Banking Corporation Limited, the Bank of China (Hong Kong) Limited and the Standard Chartered Bank (Hong Kong) Limited. See, for example, https://www.hkma.gov.hk/eng/key-functions/money/hong-kong-currency/notes/.

between April 1999 and July 2000.

On May 18, 2005, the HKMA introduced a strong-side CU to buy US dollars from licensed banks at HK$7.75, and announced the shifting of the existing weak-side Convertibility Undertaking from HK$ 7.80 to HK$ 7.85 (in small steps over a five-week period), so as to achieve symmetry around the Linked Exchange Rate of HK$7.8. The HKMA thus commits to sell (buy) Hong Kong dollars upon request by licensed banks at the strong-side (weak-side) CU.

The stability of the Hong Kong dollar exchange rate is maintained through an automatic interest rate adjustment mechanism and the firm commitment by the HKMA to honour the CUs. When the demand for Hong Kong dollars is greater (less) than the supply and the market exchange rate strengthens (weakens) to the strong-side (weak-side) CU of HK$7.75 (7.85) to one US dollar, the HKMA stands ready to sell (buy) Hong Kong dollars to banks for US dollars. The Aggregate Balance will then expand (contract) to push down (up) Hong Kong dollar interest rates, creating monetary conditions that move the Hong Kong dollar away from the strong-side (weak-side) limit to within the Convertibility Zone of 7.75 to 7.85.

Figure 2: **Interest Rates in the US and Hong Kong**



NOTE: This figure plots 3-month interbank interest rates in the US (solid blue line) and in Hong Kong (dotted red line) between January 2005 and December 2023.

There are several factors contributing to the recent pressure on the HKD-USD peg. First, the US Federal Reserve has started aggressive rate hikes since March 2022, which is evident in the steep rise in the 3-month LIBOR rate shown in Figure 2. Searching for higher yields, investors started to engage in the profitable strategy of "carry trade" by borrowing Hong Kong dollars and then sell them to buy assets in US dollars to earn higher interest rates. The resulting selling pressure causes the HKD to further depreciate.

Second, Hong Kong is still trying to recover from the economic slowdown due to the pandemic, and also from recent political turmoil exemplified by mass protests following the national security law in 2020. To support its local economy, Hong Kong banks have lagged behind US counterparts in raising interest rates. In fact, the 3-month HIBOR has actually decreased since 2022 as shown by the dotted red line in Figure 2. The divergence between US and Hong Kong interest rates further magnified the depreciationary pressure on the HKD. Only until the end of 2023 did the interest rate differential narrowed substantially.

Lastly, as one of international financial centers, Hong Kong has open market environment that permits capital to flow to and from mainland China. The free capital flows make Hong Kong appealing to foreign investors and institutions, but at the same time may exacerbate the problem of capital flight that mainland China has been facing.

3 Model

In this section we build an asset pricing model for the Hong Kong dollar (HKD) that accounts for the imperfect credibility of its peg. We derive both the equilibrium exchange rate and option prices in closed form, which allows for more efficient estimation of the model.

3.1 Setup

We assume that there is a probability p that the HKD-USD peg continues, and a probability $(1-p)$ that it ends tomorrow. If it ends, the exchange rate equals the fundamental exchange rate V_t that satisfies

$$\frac{1+r^{\$}}{1+\widetilde{r}^{H}} E_t^Q \left[V_{t+1}\right] = V_t, \tag{1}$$

where $\widetilde{r}^{H}$ denotes the interest rate in Hong Kong in the free-floating regime and $r^{\$}$ denotes the US interest rate.[10]

In the current peg regime, the HKD-USD exchange rate is constrained to be between 7.75 and 7.85. Denote the HKD-USD peg exchange rate $S^P \equiv 7.8$ and $b = 0.05$. The equilibrium exchange rate $\widetilde{S}_t$ is given by

$$\begin{aligned} \tilde{S}_t(V_t) &= \frac{1+r^{\$}}{1+r^{H}} \left[p E_t^Q H\left(\tilde{S}_{t+1}; S^P, b\right) + (1-p)\, E_t^Q V_{t+1} \right] \\ &= \frac{1+r^{\$}}{1+r^{H}} p E_t^Q H\left(\tilde{S}_{t+1}; S^P, b\right) + \frac{1+\widetilde{r}^{H}}{1+r^{H}} (1-p)\, V_t, \end{aligned} \tag{2}$$

where $E_t^Q[\cdot]$ refers to expectations under the HKD risk-neutral measure, r^H denotes the

[10] Jermann (2017) makes a similar assumption when studying the Swiss franc-Euro exchange rate.

interest rate in Hong Kong in the current peg regime, and we denote

$$H\left(x; S^P, b\right) \equiv \max\left(\min\left(x, S^P + b\right), S^P - b\right).$$

Intuitively, the current spot exchange rate is the risk-adjusted expected value of the exchange rate in the two regimes, appropriately adjusted for the interest rates. In particular, the second line is derived under the assumption in equation (1).

If the equilibrium exchange rate $\widetilde{S}_t$ falls within the band around the peg exchange rate, the observed spot exchange rate at the close is equal to $\widetilde{S}_t$. Otherwise, the spot exchange rate is equal to $\widetilde{S}_t$ truncated at the (lower or upper) boundary of the band. Therefore, the model-implied spot exchange rate at the close then equals

$$S_t^{CL} = H\left(\tilde{S}_t; S^P, b\right). \tag{3}$$

Normalizing key exchange rates by S^P, we define $\widehat{S}_t \equiv \tilde{S}_t/S^P$ and $\widehat{V}_t \equiv V_t/S^P$. As a result, the determination of equilibrium exchange rate $\tilde{S}_t$ boils down to the determination of the univariate function $\widehat{S}(\widehat{V}_t)$. Based on this, we can simplify equation (2) to

$$\begin{aligned}
\widehat{S}(\widehat{V}_t) &= \frac{\tilde{S}\left(V_t; S^P\right)}{S^P} \\
&= \frac{1+r^{\$}}{1+r^H} p E_t^Q \left[H\left(\frac{\tilde{S}\left(V_{t+1}; S^P\right)}{S^P}; 1, \frac{b}{S^P}\right)\right] + \frac{1+\widetilde{r}^H}{1+r^H}(1-p)\,\widehat{V}_t \\
&= \frac{1+r^{\$}}{1+r^H} p E_t^Q \left[H\left(\widehat{S}\left(\widehat{V}_{t+1}\right); 1, \widehat{b}\right)\right] + \frac{1+\widetilde{r}^H}{1+r^H}(1-p)\,\widehat{V}_t,
\end{aligned} \tag{4}$$

where we denote $\widehat{b} \equiv \frac{b}{S^P} = \frac{0.05}{7.8}$=0.0064. For ease of notation from now on we simply write $H(\widehat{S}(\widehat{V}_{t+1}); 1, \widehat{b})$ as $H(\widehat{S}(\widehat{V}_{t+1}))$. That is,

$$\widehat{S}(\widehat{V}_t) = \frac{1+r^{\$}}{1+r^H} p E^Q \left[H\left(\widehat{S}(\widehat{V}_{t+1})\right)\right] + \frac{1+\widetilde{r}^H}{1+r^H}(1-p)\,\widehat{V}_t. \tag{5}$$

We can derive the equilibrium exchange rate $\widehat{S}(\widehat{V}_t)$ in closed form when we cast the model in continuous time. Specifically, under the HKD risk-neutral measure Q, the dynamics of the fundamental exchange rate V_t in continuous time is given below:

$$\begin{aligned}
\frac{dV_t}{V_t} &= \left(\widetilde{r}_{HKD} - r_{USD}\right) dt + \sigma_V dW_{V,t} \\
&\equiv \mu_V dt + \sigma_V dW_{V,t},
\end{aligned} \tag{6}$$

where $W_{V,t}$ is independent Brownian motions under the measure Q, and $\mu_V \equiv \widetilde{r}_{HKD} - r_{USD}$ with $\widetilde{r}_{HKD}$ and r_{USD} being instantaneous interest rates for the HKD and the USD, respectively. Let Δt denote the length of a period in discrete time. Then the per-period interest rates in the preceding discrete-time setup satisfy: $1+r^{\$} = \exp(r_{USD}\Delta t)$ and $1+\widetilde{r}^{H} = \exp(\widetilde{r}_{HKD}\Delta t)$. The drift in the above equation is specified so as to exclude any arbitrage opportunities. Similarly, the per-period probability $p = \exp(-\lambda\Delta t)$ while we assume that the current managed floating regime will be abandoned upon arrival of a Poisson process with intensity λ.

To ensure the existence of a solution to equation (5), we assume that $\frac{1+r^{\$}}{1+r^{H}}p < 1$, which can be rewritten as equation (7) in Assumption 1. Note that the right-hand side of equation (5) can be considered as an operator on the equilibrium exchange rate. The condition (7) in Assumption 1 satisfies Blackwell's sufficient conditions for a contraction mapping, which guarantees the existence of a fixed point.

Assumption 1 *We assume*

$$\lambda + r_{HKD} - r_{USD} > 0. \tag{7}$$

Next, we impose the following assumption such that the Hong Kong interest rate in the current peg regime equals the counterpart in the free-floating regime: $r_{HKD} = \widetilde{r}_{HKD}$.

Assumption 2 *We assume*

$$\mu_V = r_{HKD} - r_{USD}. \tag{8}$$

In the proposition below, we derive the equilibrium exchange rate in closed form.

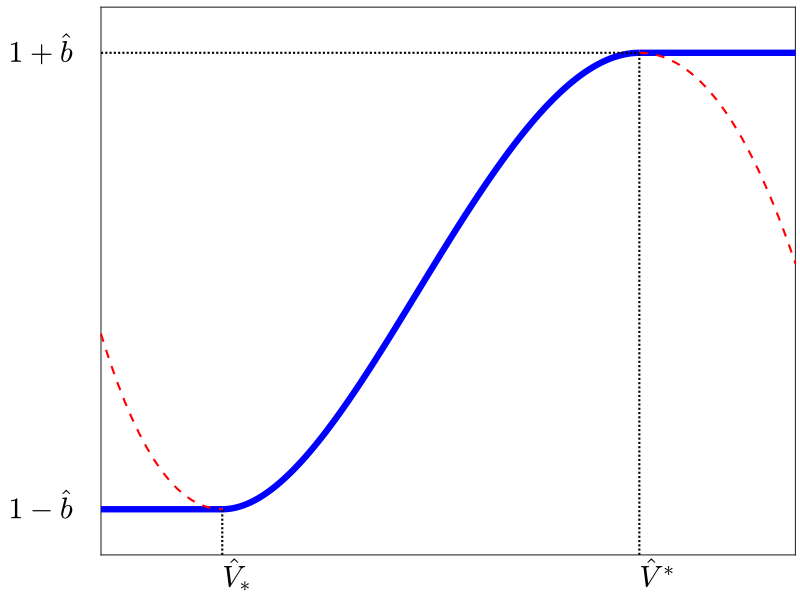
Proposition 1 *In the continuous-time model, the scaled equilibrium exchange rate $\widehat{S}(\widehat{V}_t)$ is determined as follows:*

$$\widehat{S}(\widehat{V}) = \begin{cases} 1 - \widehat{b}, & \text{if } \widehat{V} \leq \widehat{V}_*; \\ C_0\widehat{V} + C_1\widehat{V}^{\eta_1} + C_2\widehat{V}^{\eta_2}, & \text{if } \widehat{V}_* < \widehat{V} < \widehat{V}^*; \\ 1 + \widehat{b}, & \text{if } \widehat{V} \geq \widehat{V}^*, \end{cases} \tag{9}$$

where the thresholds $\widehat{V}_*$ and $\widehat{V}^*$ are endogenously determined and the expressions of η_1, η_2, and C_0 through C_2 are given in the proof in the appendix. Under Assumption 2, $C_0 = 1$.

Proof. See Appendix A. ■

Figure 3: **Equilibrium Exchange Rate**



NOTE: This figure plots the equilibrium exchange rate as a function of the (scaled) fundamental value.

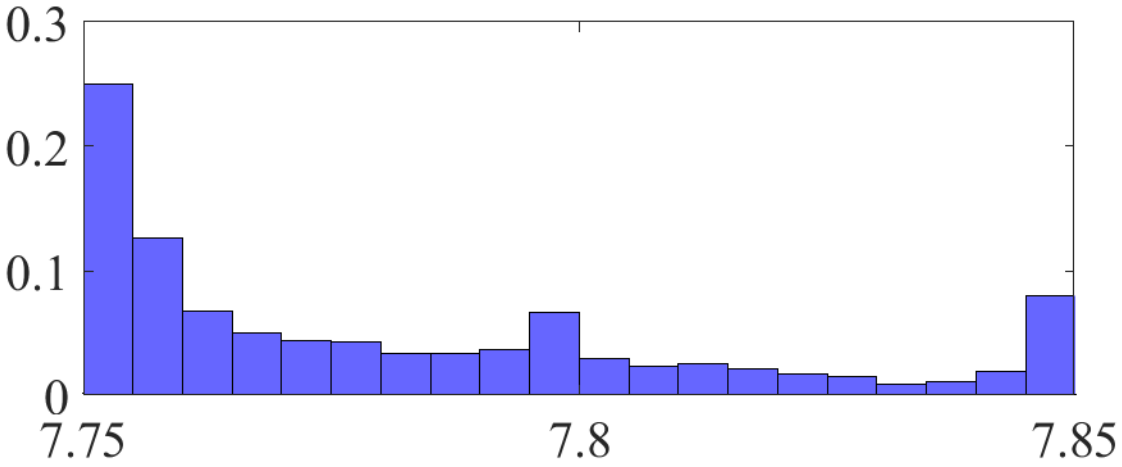
Based on our estimation results, we find that $\widehat{S}(\widehat{V}_t)$ has the S shape in the middle range when $\widehat{V}$ falls within the interval between $\widehat{V}_*$ and $\widehat{V}^*$. Figure 3 plots the equilibrium exchange rate $\widehat{S}(\widehat{V}_t)$. Mathematically, under Assumption 1 the exponents η_1 and η_2 in equation (9) have opposite signs. Without loss of generality, suppose $\eta_1 > 0 > \eta_2$ and thus $C_1 < 0 < C_2$. Intuitively, as the fundamental rate deviates from the central parity in the positive direction, $\widehat{V}_t$ increases, so does the term $\widehat{V}^{\eta_1}$. When $\widehat{V}$ gets closer to $\widehat{V}^*$, the shape of $\widehat{S}$ gets flatter because of expected interventions in the near future. This is reminiscent of the exchange rate behavior in a target-zone model (see Krugman, 1991) that the expectation of possible interventions affects exchange rate behavior even when the exchange rate lies inside the zone.

3.2 Exchange Rate Distribution

The empirical distribution of the USD-HKD exchange rate is U-shaped in the data, as shown in Figure 4. The U-shaped distribution is at odds with the bell-shaped distribution under standard Black-Scholes models. In sharp contrast, our model implies a distribution that closely resembles the empirical one in the data as we show below.

In our model, with probability $e^{-\lambda\tau}$, the current regime remains in place at $t+\tau$. Depending on whether the (scaled) exchange rate, $\widehat{S}_{t+\tau}$, hits one of the boundaries or remains strictly within the band, there are three possibilities: (i) with probability $1-\Phi\left(-d^*\right)=\Phi\left(d^*\right)$, $\widehat{S}_{t+\tau}$

Figure 4: **Histogram of Historical USDHKD Exchange Rate**



NOTE: This figure plots the empirical distribution of the daily USD-HKD exchange rate between January 2007 and December 2023.

is equal to its upper bound $1+\widehat{b}$; (ii) with probability $\Phi\left(-d_*\right)$, it is equal to the lower bound $1-\widehat{b}$; and (iii) with probability $\Phi\left(-d^*\right)-\Phi\left(-d_*\right)$, it is equal to $C_0\widehat{V}_{t+\tau}+C_1\widehat{V}_{t+\tau}^{\eta_1}+C_2\widehat{V}_{t+\tau}^{\eta_2}$, where

$$d^* \equiv \frac{\log\left(\widehat{V}_t/\widehat{V}^*\right)+\left(\mu_V-\frac{1}{2}\sigma_V^2\right)\tau}{\sigma_V\sqrt{\tau}}, \tag{10}$$

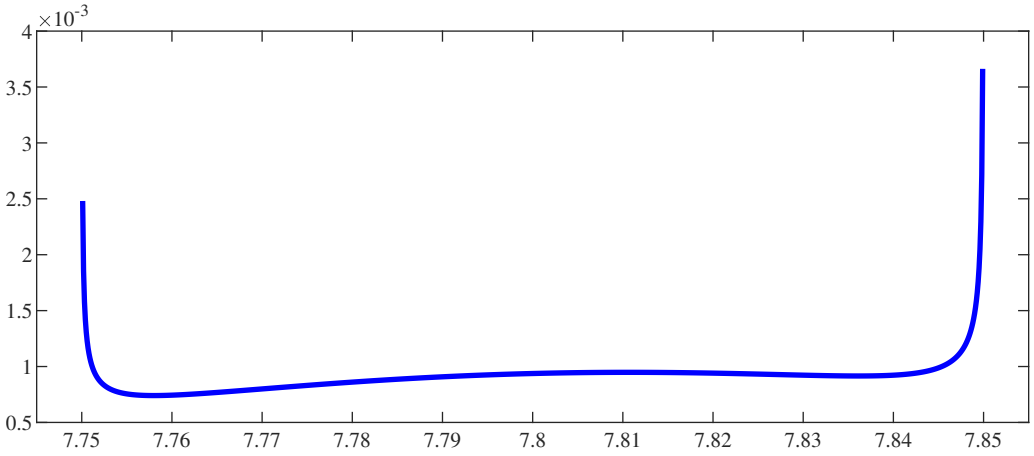
$$d_* \equiv \frac{\log\left(\widehat{V}_t/\widehat{V}_*\right)+\left(\mu_V-\frac{1}{2}\sigma_V^2\right)\tau}{\sigma_V\sqrt{\tau}}. \tag{11}$$

and $\widehat{V}_*$ and $\widehat{V}^*$ are defined in Proposition 1. In the last possibility, when the (scaled) fundamental value is between $\widehat{V}_*$ and $\widehat{V}^*$, the probability density function of the exchange rate within the band can be derived by a change of variable

$$f^{TZ}\left(\widehat{S}_{t+\tau}\right)=\frac{LN_{\left(\widehat{V}_*,\widehat{V}^*\right)}\left(\widehat{V}_{t+\tau}\right)}{\widehat{S}'\left(\widehat{V}_{t+\tau}\right)}=\frac{\exp\left(-\frac{\left(\ln\left(\widehat{V}_{t+\tau}/\widehat{V}_t\right)-\left(\mu_V-\frac{1}{2}\sigma_V^2\right)\tau\right)^2}{2\sigma_V^2\tau}\right)}{\sigma_V\sqrt{2\pi\tau}\widehat{V}_{t+\tau}\widehat{S}'\left(\widehat{V}_{t+\tau}\right)}1_{\left\{\widehat{V}_{t+\tau}\in\left(\widehat{V}_*,\widehat{V}^*\right)\right\}}, \tag{12}$$

where $LN_{\left(\widehat{V}_*,\widehat{V}^*\right)}(\widehat{V}_{t+\tau})$ denotes a truncated log-normal distribution between $\widehat{V}_*$ and $\widehat{V}^*$, and $\widehat{V}_{t+\tau}=\widehat{S}^{-1}(\widehat{S}_{t+\tau})$. It is straightforward to see that the integral of $f^{TZ}(\widehat{S}_{t+\tau})$ from $1-\widehat{b}$ to $1+\widehat{b}$ equals $\Phi\left(-d^*\right)-\Phi\left(-d_*\right)$. Figure 5 plots $f^{TZ}(\widehat{S}_{t+\tau})$ within the band for $\widehat{S}_{t+\tau}\in(1-\widehat{b},1+\widehat{b})$.

Figure 5: **Model-implied Distribution within the Band**



NOTE: This figure plots the model-implied density distribution of the equilibrium exchange rate within the band in the current regime (i.e., $f^{TZ}(\widehat{S}_{t+\tau})$ in equation (12)).

With probability $1-e^{-\lambda\tau}$, the economy is in the free-floating regime at $t+\tau$ in which the (scaled) exchange rate at $t+\tau$ is equal to the fundamental value: $\widehat{S}_{t+\tau}=\widehat{V}_{t+\tau}$, which follows a log-normal distribution with mean $\ln\widehat{V}_t+\left(\mu_V-\frac{1}{2}\sigma_V^2\right)\tau$ and variance $\sigma_V^2\tau$, since $\widehat{V}_{t+\tau}=\widehat{V}_t\exp\left(\left(\mu_V-\frac{1}{2}\sigma_V^2\right)\tau+\sigma_V\sqrt{\tau}z_V\right)$ where z_V follows a standard normal distribution. That is, conditional on the regime being the free-floating one, the probability density function of $\widehat{S}_{t+\tau}$, which equals $\widehat{V}_{t+\tau}$, is given by

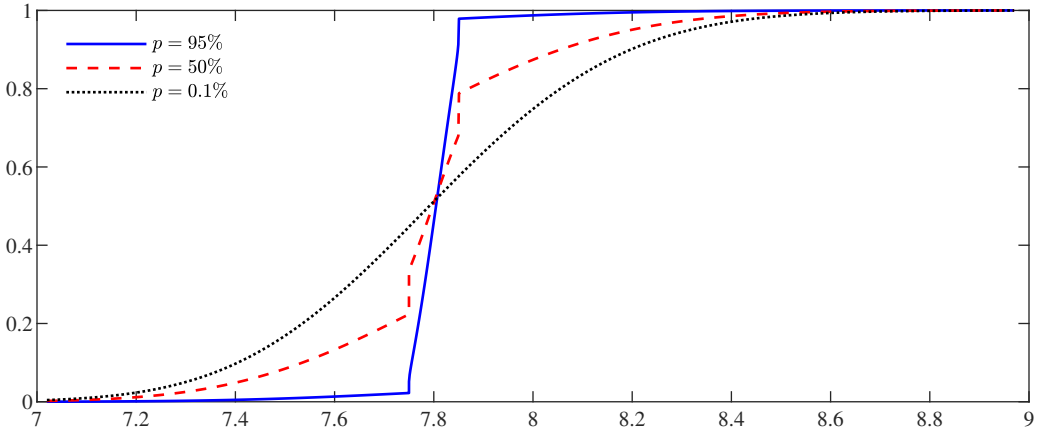
$$f^{FF}\left(\widehat{S}_{t+\tau}\right)=LN\left(\widehat{V}_{t+\tau}\right)=\frac{\exp\left(-\frac{\left(\ln\left(\widehat{V}_{t+\tau}/\widehat{V}_t\right)-\left(\mu_V-\frac{1}{2}\sigma_V^2\right)\tau\right)^2}{2\sigma_V^2\tau}\right)}{\sigma_V\sqrt{2\pi\tau}\widehat{V}_{t+\tau}}, \tag{13}$$

where $LN(\widehat{V}_{t+\tau})$ denotes the above log-normal distribution.

Taking into account possible regime shifts, Figure 6 plots the complete density function for three cases: 1) $\lambda=25$ (or $p=0.2\%$); 2) $\lambda=10$ (or $p=8.2\%$); and 3) $\lambda=0.2$ (or $p=95.1\%$). The distribution function in the first case closely mirrors the log-normal distribution assumed in standard Black-Scholes models. This resemblance arises from the high likelihood in the first case that the existing regime will transition to a free-floating one. Consequently, this scenario tends to overstate the probability of the exchange rate breaking out of the band compared with the other two more realistic cases.

In contrast, the third case, which represents the model-implied density for an average day in the data, takes into account the possibility of the regime switching to the free-floating one. However, it assesses a substantial likelihood for the current regime to persist. Therefore, in

Figure 6: **Model-implied Full Cumulative Distribution Function**



NOTE: This figure plots the full cumulative distribution function of the model-implied equilibrium exchange rate.

this latter case, the exchange rate predominantly fluctuates within the band, though there exists a non-trivial probability of it breaking out. In the next section, we will use our estimation results to further investigate this important implication.

3.3 Forward and Option Pricing

We estimate the model to match the spot rate and four options. In this subsection, we price HKD forwards and options in closed form.

First, let $F(\tau) \equiv E_t^Q\left[S_{t+\tau}^{CL}\right]$ denote the forward rate, which is defined as the date-t conditional expectation of the HKD's spot rate at date $t+\tau$. Suppose there are N periods until $t+\tau$; that is, $N = \tau/\Delta t$. In the proposition below, we provide closed-form formula for the HKD forward rate.

Proposition 2 *Under the model, the HKD forward rate has the following closed-form formula:*

$$\begin{aligned} F(\tau) &= p^N E_t^Q\left[H\left(\widetilde{S}_{t+\tau}; S^P, b\right)\right] + \left(1-p^N\right) E_t^Q\left[V_{t+\tau}\right] \\ &\equiv p^N F_S(\tau) + \left(1-p^N\right) F_V(\tau), \end{aligned}$$

where

$$\begin{aligned} F_S(\tau) &\equiv E_t^Q\left[H\left(\widetilde{S}_{t+\tau}; S^P, b\right)\right] \\ &= \left(1-\Phi\left(-d^*\right)\right)\left(S^P+b\right)+\Phi\left(-d_*\right)\left(S^P-b\right) \\ &\quad +\left(\Phi\left(-d^*\right)-\Phi\left(-d_*\right)\right)S^P\sum\nolimits_{i=0}^{2}C_i\Gamma\left(\widehat{V}_t;\eta_i\right), \end{aligned} \tag{14}$$

and

$$F_V(\tau) \equiv E_t^Q\left[V_{t+\tau}\right] = V_t\exp\left(\mu_V\tau\right), \tag{15}$$

and

$$\Gamma(\widehat{V}_t;\eta) = \widehat{V}_t^{\eta}e^{\eta\mu_V\tau+\frac{1}{2}\eta(\eta-1)\sigma_V^2\tau}\frac{\Phi\left(-d^*-\eta\sigma_V\sqrt{\tau}\right)-\Phi\left(-d_*-\eta\sigma_V\sqrt{\tau}\right)}{\Phi\left(-d^*\right)-\Phi\left(-d_*\right)}. \tag{16}$$

Proof. See Appendix A. ■

Next, we turn to pricing options. Consider a call option with strike K and maturity τ. Its option price is given by

$$\begin{aligned} & C(K,\tau) \\ = \;& p^N e^{-r_{HKD}\tau}E^Q\left[\max\left(H\left(\widetilde{S}_{t+\tau};S^P,b\right)-K,0\right)\right] \\ & +\sum\nolimits_{n=1}^{N}p^{n-1}(1-p)\,e^{-r_{HKD}n\Delta t-\widetilde{r}_{HKD}(N-n)\Delta t}E^Q\left[\max\left(V_{t+\tau}-K,0\right)\right] \\ \equiv \;& p^N C_S(K,\tau)+\left(1-p^N\right)\chi C_V(K,\tau), \end{aligned} \tag{17}$$

where $\chi \equiv \frac{1}{1-p^N}\sum_{n=1}^{N}p^{n-1}(1-p)\,e^{-r_{HKD}n\Delta t+\widetilde{r}_{HKD}n\Delta t} = 1$ under Assumption 2, and

$$\begin{aligned} C_S(K;\tau) &\equiv e^{-r_{HKD}\tau}E_t^Q\left[\max\left(H\left(\widetilde{S}_{t+\tau};S^P,b\right)-K,0\right)\right], \\ C_V(K;\tau) &\equiv e^{-\widetilde{r}_{HKD}\tau}E_t^Q\left[\max\left(V_{t+\tau}-K,0\right)\right]. \end{aligned}$$

In the following proposition, we derive closed-form formula for the above option price.

Proposition 3 *The price of a call option with strike K and maturity τ is a weighted average of two components $C_S(K,\tau)$ and $C_V(K,\tau)$ as shown in equation (17).*

(i) The component $C_V(K,\tau)$ has the following Black-Scholes formula:

$$C_V(K,\tau) \equiv e^{-\widetilde{r}_{HKD}\tau}E_t^Q\max\left[V_{t+\tau}-K,0\right] = e^{-r_{USD}\tau}V_t\Phi\left(d_{1,V}\right)-e^{-\widetilde{r}_{HKD}\tau}K\Phi\left(d_{2,V}\right), \tag{18}$$

where

$$d_{1,V} = d_{2,V} + \sigma_V \sqrt{\tau} = \frac{\log\left(V_t/K\right) + \left(\mu_V + \frac{1}{2}\sigma_V^2\right)\tau}{\sigma_V \sqrt{\tau}}, \tag{19}$$

$$d_{2,V} = \frac{\log\left(V_t/K\right) + \left(\mu_V - \frac{1}{2}\sigma_V^2\right)\tau}{\sigma_V \sqrt{\tau}}. \tag{20}$$

(ii) The component $C_S\left(K,\tau\right)$ is given by:

$$C_S\left(K,\tau\right) = \begin{cases} 0, & \text{if } K \geq S^P + b \\ e^{-r_{HKD}\tau}\left(F_S\left(\tau\right) - K\right), & \text{if } K \leq S^P - b \\ \left[\begin{array}{c} \left(1 - \Phi\left(-d^*\right)\right) e^{-r_{HKD}\tau}\left[S^P + b - K\right] \\ + \left(\Phi\left(-d^*\right) - \Phi\left(-d_*\right)\right) e^{-r_{HKD}\tau} \\ \times \left[S^P \sum_{i=0}^{2} C_i \Gamma^*\left(\widehat{V}_t; \eta_i\right) - K\Gamma^*\left(\widehat{V}_t; 0\right)\right] \end{array}\right], & \text{otherwise} \end{cases} \tag{21}$$

where

$$\Gamma^*(\widehat{V}_t;\eta) \equiv \widehat{V}_t^{\eta} e^{\eta\mu_V\tau + \frac{1}{2}\left(\eta^2 - \eta\right)\sigma_V^2\tau} \frac{\Phi\left(-d^* - \eta\sigma_V\sqrt{\tau}\right) - \Phi\left(-d_K - \eta\sigma_V\sqrt{\tau}\right)}{\Phi\left(-d^*\right) - \Phi\left(-d_*\right)},$$

$$d_K \equiv \frac{\log\left(\widehat{V}_t/\widehat{V}_K\right) + \left(\mu_V - \frac{1}{2}\sigma_V^2\right)\tau}{\sigma_V\sqrt{\tau}},$$

and $\widehat{V}_K$ is the cutoff value satisfying $\widehat{S}(\widehat{V}_K) = \widehat{K}\left(\equiv K/S^P\right)$, which has a unique solution when $\widehat{K} \in [1 - \widehat{b}, 1 + \widehat{b}]$.

Proof. See Appendix A. ■

We can similarly derive the closed-form formula for the price of a put option with the same strike and maturity.

$$P\left(K,\tau\right) \equiv p^N P_S\left(K,\tau\right) + \left(1 - p^N\right)\chi P_V\left(K,\tau\right), \tag{22}$$

where

$$P_V\left(K,\tau\right) = e^{-\widetilde{r}_{HKD}\tau} E_t^Q \max\left[K - V_{t+\tau}, 0\right] = -V_t e^{-r_{USD}\tau} N\left(-d_{1,V}\right) + K e^{-\widetilde{r}_{HKD}\tau} N\left(-d_{2,V}\right),$$

and

$$P_S(K,\tau) = \begin{cases} e^{-r_{HKD}\tau}\left(K - F_S(\tau)\right), & \text{if } K \geq S^P + b; \\ 0, & \text{if } K \leq S^P - b; \\ \left[\begin{array}{c} \Phi(-d_*)\, e^{-r_{HKD}\tau}\left[K - \left(S^P - b\right)\right] \\ + \left(\Phi(-d^*) - \Phi(-d_*)\right) e^{-r_{HKD}\tau} \\ \times \left[K\Gamma_*\left(\widehat{V}_t; 0\right) - S^P \sum_{i=0}^{2} C_i \Gamma_*\left(\widehat{V}_t; \eta_i\right)\right] \end{array}\right], & \text{otherwise,} \end{cases} \tag{23}$$

and

$$\Gamma_*(\widehat{V}_t;\eta) \equiv \widehat{V}_t^{\eta} e^{\eta\mu_V\tau + \frac{1}{2}(\eta^2-\eta)\sigma_V^2\tau} \frac{\Phi(-d_K - \eta\sigma_V\sqrt{\tau}) - \Phi(-d_* - \eta\sigma_V\sqrt{\tau})}{\Phi(-d^*) - \Phi(-d_*)}.$$

4 Model Estimation and Results

In this section, we describe estimation methodology and results.

4.1 Data

Our sample period is from 2007 to 2023. We obtain most data at a daily frequency from Bloomberg, such as, the historical USD-HKD exchange rate, the 3-month Hong Kong interbank offer rate (HIBOR) for the HKD and London interbank offer rate (LIBOR) for the USD, and derivatives data. The derivatives data include forwards/futures and options written on the HKD.

The HKD option data consist of implied volatility quotes for at-the-money options ("ATM"), risk reversals ("RR"), and butterfly spreads ("BY"), with a maturity of 3 months. The RR and BY quotes are available for strike prices corresponding to 25% and 10% delta (labeled as "25Δ" and "10Δ" respectively). These quotes can then be used to infer implied volatilities of 25Δ or 10Δ options by the standard approach (e.g., see Bisesti et al., 2005; Jermann, 2017, for more details). For 25Δ calls and puts, for instance, implied volatilities are computed as

$$\begin{aligned} \sigma_{25C} &= \sigma_{ATM} + \sigma_{25BY} + \frac{1}{2}\sigma_{25RR}, \\ \sigma_{25P} &= \sigma_{ATM} + \sigma_{25BY} - \frac{1}{2}\sigma_{25RR}. \end{aligned}$$

Following the quoting convention of the RMB options markets, the Black-Scholes formula is then used to compute the prices and strike prices corresponding to 25Δ and 10Δ options. In the end, we obtain four option price series: two for puts and two for calls.

Table 1: Summary Statistics of HKD Option Prices

	strike				price	IV
	mean	25%	50%	75%	mean	mean
Put (10Δ)	7.68	7.65	7.68	7.72	0.37	2.00
Call (10Δ)	7.85	7.82	7.85	7.88	0.27	1.48
Put (25Δ)	7.75	7.73	7.74	7.77	0.70	1.20
Call (25Δ)	7.80	7.78	7.80	7.83	0.54	0.93

NOTE: This table presents summary statistics for strike prices, option prices, and implied volatility (expressed as percentages) for four HKD options spanning the period from 2007 to 2023. We provide the average strike price along with the 25th, 50th, and 75th percentiles for strike prices. Additionally, we report the average option prices and implied volatilities.

Table 1 reports summary statistics for HKD options for these four options during the sample period. As shown in Table 1, the 10Δ put options have an average strike of 7.68. Interestingly, these strike prices are lower than the strong-side CU of 7.75 for more than 75% of the time. Similarly, the strike prices for the 10Δ call options are greater than the weak-side CU of 7.85 for about half of the time. Given that that our main interest is in the implied probabilities of exchange rate realizations breaking out the convertibility zone, it is useful that our data include options with strike prices that are typically outside the convertibility zone.

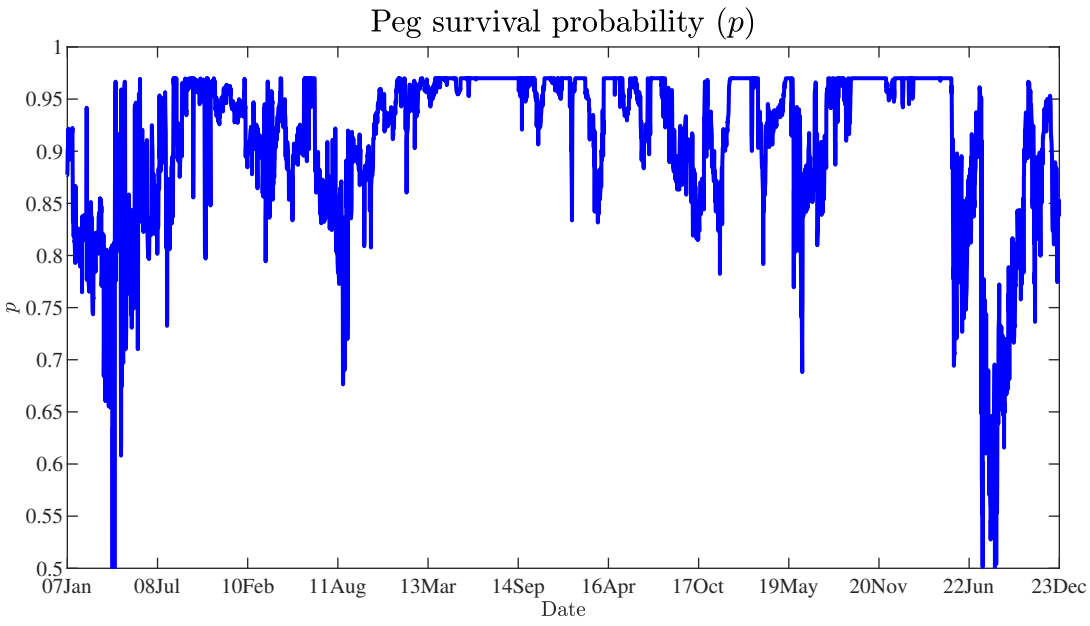
The model is used to estimate the values for (V, p, σ_V) that best fit the spot rate and the prices of the four three-month HKD options. Interest rates are taken as given from the data. Goodness of fit is represented by the sum of squared deviations between the prices (for the options and the exchange rate) from the model and the data. As the benchmark, the deviations are equally weighted. We repeat this procedure for every day of the sample to produce time series for the estimates of $(V_t, p_t, \sigma_{V,t})$.

4.2 Results

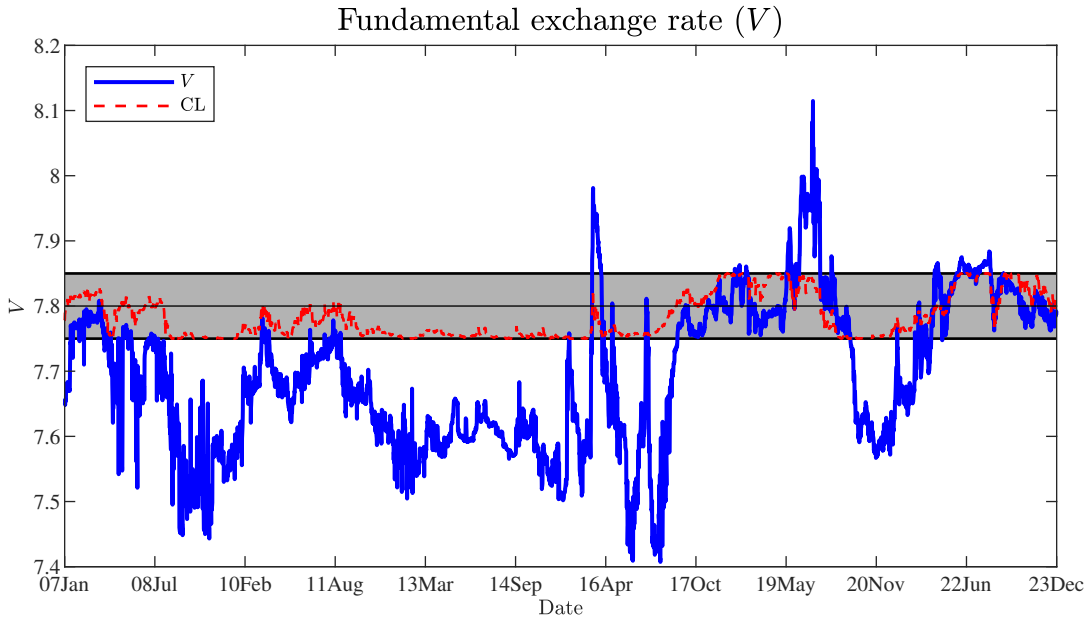
We present the empirical results in this subsection. Figure 7 illustrates the main estimation results. The first panel (Figure 7a) displays the estimated probability, p, that the HKD peg remains intact. At several key stress points, this probability experiences significant declines. Notably, it dropped to 69% in August 2019 when China's currency renminbi (RMB) weakened past 7 per USD amid the US-China trade war. It further declined to 50% in late 2022, coinciding with rising U.S. interest rates and declining interbank liquidity.[11] Such an

[11]The interbank liquidity dropped from more than 300 billion HKD in March 2022 to about 50 billion HKD in April 2023.

Figure 7: **Estimation Results**



(a)



(b)

NOTE: Blue line in Panel (a) plots the 3-month probability p that the HKD peg remains credible in 90 days. The red line is the spot USD-HKD exchange rate. The shaded area is the band set for the USD-HKD exchange rate. Panel (b) plots the estimated fundamental exchange rate value V.

elevated risk of the peg breaking, as viewed by financial markets, had not been observed since the global financial crisis.

The second panel (Figure 7b) plots the estimated fundamental exchange rate value, V, over time. The fluctuations in V are considerably wider than the band, particularly during major financial and geopolitical events. For example, the estimated value of V increased during periods of economic uncertainty, including the US-China trade war and the COVID-19 pandemic, indicating increased depreciatory pressure on the HKD. Additionally, the estimated volatility of the fundamental exchange rate (not reported here but available upon request) closely tracks the option-implied volatility.

The figure highlights the interplay between global monetary conditions and market confidence in the peg. The estimates depend on factors such as the spot exchange rate, option-implied volatilities, and interest rate differentials between Hong Kong and the U.S. Regression analysis suggests that these variables collectively explain about 25% of the variation in the fundamental exchange rate and 13% of the variation in the peg continuation probability. Notably, option-implied volatility (particularly the 10-delta butterfly spread) emerges as a crucial predictor, with its exclusion significantly reducing explanatory power. These findings underscore the importance of liquidity conditions, U.S. monetary policy, and exchange rate expectations in shaping the credibility of Hong Kong's currency board arrangement.

Our estimates depend on not only the spot exchange rate and option implied volatility, but also the interest rates in Hong Kong and the US. To examine the relative importance of these input variables in the estimation, we run regressions of daily changes in the estimated fundamental value (i.e., $\Delta log(V_t)$) on these input variables. The regression results are reported in Table 2. The regression results for daily changes in the estimated continuation probability (i.e., $\Delta log(p_t)$) are reported in Table 3.

The results in these two tables indicate that all input variables play a significant role in our estimation. Collectively, they account for about 25% of the variation in changes in the estimated fundamental value, and 13% of the variation in the estimated continuation probability (Columns (1) in Tables 2 and 3). The relatively low R^2 in these regressions reflects the nonlinear, regime-switching nature of the model—the HKD is closer to either end of the trading band when market uncertainty about the peg's sustainability rises.

Individually, the most important input variable is the implied-volatility for $10-\Delta$ butterfly spreads (i.e., $\Delta\sigma_{10BY}$). Specifically, dropping this variable reduces R^2 from 25% to 11% for changes in estimated fundamental value (Column (2)) in Table 2), and from 13% to 6% for changes in estimated continuation probability (Column (2)) in Table 3).

Table 2: Sensitivity Analysis: V

	(1)	(2)	(3)	(4)	(5)	(6)	(7)	(8)	(9)
Δi^{HKD}	0.02***	0.02***	0.02***	0.02***	0.02***	0.02***	0.02***	0.01***	
	(0.00)	(0.00)	(0.00)	(0.00)	(0.00)	(0.00)	(0.00)	(0.00)	
Δi^{USD}	−0.01***	−0.02***	−0.01***	−0.01***	−0.01***	−0.01***	−0.01**		0.00
	(0.00)	(0.00)	(0.00)	(0.00)	(0.00)	(0.00)	(0.00)		(0.00)
ΔS^{CL}	0.32***	0.34***	0.32***	0.32***	0.33***	0.32***		0.31***	0.30***
	(0.03)	(0.04)	(0.03)	(0.03)	(0.03)	(0.03)		(0.03)	(0.03)
$\Delta\sigma_{ATM}$	0.01***	0.02***	0.01***	0.01***	0.01***		0.01***	0.01***	0.01***
	(0.00)	(0.00)	(0.00)	(0.00)	(0.00)		(0.00)	(0.00)	(0.00)
$\Delta\sigma_{25RR}$	0.02***	0.02***	0.01***	0.02***		0.02***	0.02***	0.02***	0.02***
	(0.00)	(0.00)	(0.00)	(0.00)		(0.00)	(0.00)	(0.00)	(0.00)
$\Delta\sigma_{25BY}$	−0.01***	0.05***	−0.01***		−0.01***	−0.01**	−0.01**	−0.01***	−0.01***
	(0.00)	(0.00)	(0.00)		(0.00)	(0.00)	(0.00)	(0.00)	(0.00)
$\Delta\sigma_{10RR}$	−0.01***	−0.01***		−0.01***	0.00***	−0.01***	−0.01***	−0.01***	−0.01***
	(0.00)	(0.00)		(0.00)	(0.00)	(0.00)	(0.00)	(0.00)	(0.00)
$\Delta\sigma_{10BY}$	0.04***		0.04***	0.04***	0.04***	0.04***	0.04***	0.04***	0.04***
	(0.00)		(0.00)	(0.00)	(0.00)	(0.00)	(0.00)	(0.00)	(0.00)
Obs.	4130	4130	4130	4130	4130	4130	4130	4130	4130
adj. R^2(%)	24.5	10.5	24.2	24.4	23.7	23.9	22.9	24.3	23.7

NOTE: This table reports results from regressions of daily changes in the fundamental value (i.e., $\Delta log(V_t)$). Independent variables include daily changes in Hong Kong interest rate (Δi^{HKD}), US interest rate (Δi^{USD}), implied volatility quotes for at-the-money options ($\Delta\sigma_{ATM}$), risk-reversals ($\Delta\sigma_{25RR}$ or $\Delta\sigma_{10RR}$), and butterfly spreads ($\Delta\sigma_{25BY}$ or $\Delta\sigma_{10BY}$). Column (1) reports the results from the regression with all the above regressors, while Columns (2)-(9) report the results with one regressor dropped at a time. Significance levels: * $p < .10$; ** $p < .05$; and *** $p < .01$.

Table 3: Sensitivity Analysis: p

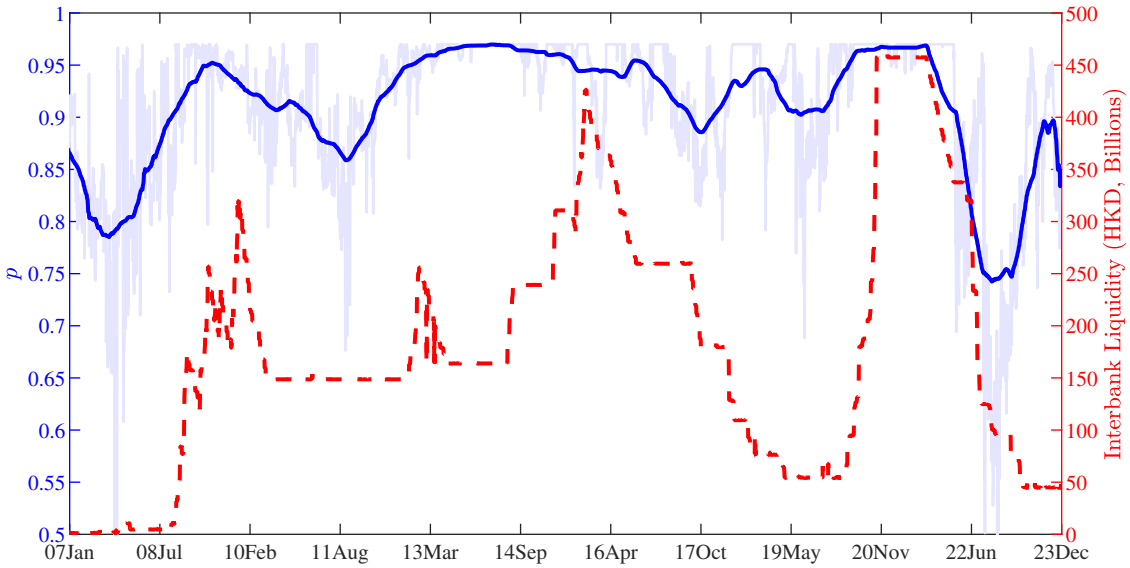
	(1)	(2)	(3)	(4)	(5)	(6)	(7)	(8)	(9)
Δi^{HKD}	0.07***	0.07***	0.06***	0.07***	0.07***	0.06***	0.06***	0.05***	
	(0.01)	(0.01)	(0.01)	(0.01)	(0.01)	(0.01)	(0.01)	(0.01)	
Δi^{USD}	−0.06***	−0.07***	−0.06***	−0.07***	−0.06***	−0.06***	−0.05**		−0.01
	(0.02)	(0.02)	(0.02)	(0.02)	(0.02)	(0.02)	(0.02)		(0.02)
ΔS^{CL}	0.97***	1.03***	0.94***	0.95***	1.00***	1.00***		0.94***	0.89***
	(0.17)	(0.17)	(0.17)	(0.17)	(0.17)	(0.17)		(0.17)	(0.17)
$\Delta\sigma_{ATM}$	−0.11***	−0.09***	−0.12***	−0.12***	−0.11***		−0.11***	−0.11***	−0.11***
	(0.01)	(0.01)	(0.01)	(0.01)	(0.01)		(0.01)	(0.01)	(0.01)
$\Delta\sigma_{25RR}$	0.06***	0.08***	−0.04***	0.06***		0.06***	0.06***	0.06***	0.06***
	(0.01)	(0.01)	(0.01)	(0.01)		(0.01)	(0.01)	(0.01)	(0.01)
$\Delta\sigma_{25BY}$	−0.24***	−0.05**	−0.25***		−0.24***	−0.26***	−0.24***	−0.24***	−0.24***
	(0.02)	(0.02)	(0.02)		(0.02)	(0.02)	(0.02)	(0.02)	(0.02)
$\Delta\sigma_{10RR}$	−0.07***	−0.07***		−0.07***	−0.04***	−0.07***	−0.07***	−0.07***	−0.07***
	(0.01)	(0.01)		(0.01)	(0.00)	(0.01)	(0.01)	(0.01)	(0.01)
$\Delta\sigma_{10BY}$	0.12***		0.13***	0.08***	0.13***	0.11***	0.13***	0.12***	0.12***
	(0.01)		(0.01)	(0.01)	(0.01)	(0.01)	(0.01)	(0.01)	(0.01)
Obs.	4130	4130	4130	4130	4130	4130	4130	4130	4130
adj. R^2(%)	13.0	6.1	11.3	10.3	12.6	10.2	12.3	12.8	12.5

NOTE: This table reports results from regressions of daily changes in the continuation probability (i.e., $\Delta log(p_t)$). Independent variables include daily changes in Hong Kong interest rate (Δi^{HKD}), US interest rate (Δi^{USD}), implied volatility quotes for at-the-money options ($\Delta\sigma_{ATM}$), risk-reversals ($\Delta\sigma_{25RR}$ or $\Delta\sigma_{10RR}$), and butterfly spreads ($\Delta\sigma_{25BY}$ or $\Delta\sigma_{10BY}$). Column (1) reports the results from the regression with all the above regressors, while Columns (2)-(9) report the results with one regressor dropped at a time. Significance levels: * $p < .10$; ** $p < .05$; and *** $p < .01$.

4.2.1 Sustainability of the current peg regime

Figure 8 plots the smoothed probability based on our estimation results. As shown by the solid blue line in the figure, the estimated probability drops to around 60% in March 2022 when the Federal Reserve started the tightening cycle. At the same time, interbank liquidity (the dashed red line) drops from more than 300 billion HKD in March 2022 to about 50 billion HKD in April 2023.

Figure 8: **Market-based Measure of the Continuation Probability**

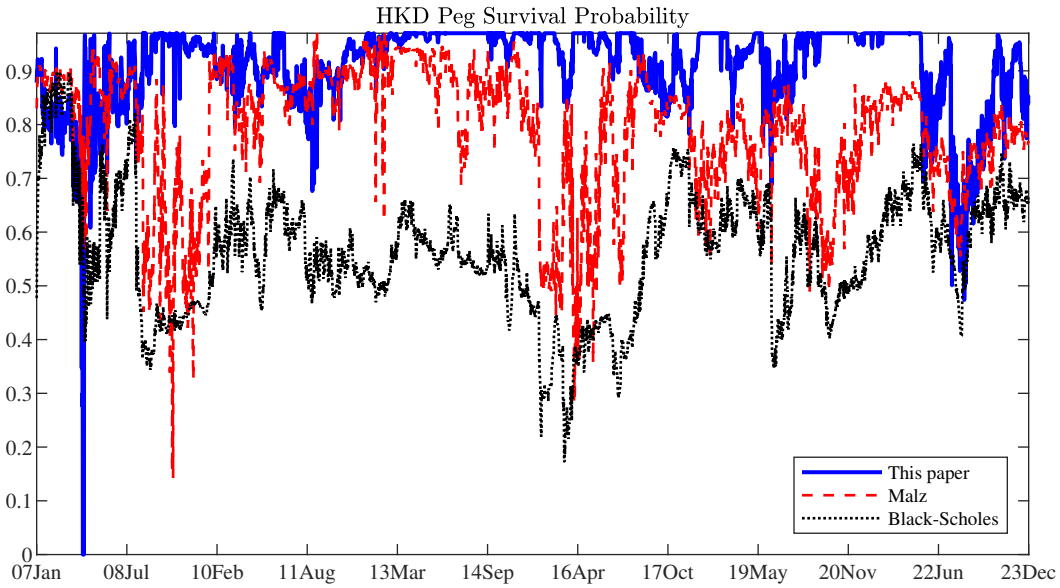


NOTE: Solid blue line shows the smoothed 3-month probability as the moving average over 250 days. The light blue line is the estimated 3-month probability as in Figure 7. Dashed red line shows the interbank liquidity.

As discussed earlier, the Black-Scholes model tend to overstate the probability of breaking out the band. This finding is confirmed by Figure 9 by the large gap between the estimates based on the Black-Scholes model and our model. As shown by the dotted black line, ignoring possible regime shifts, the Black-Scholes model assigns an average probability of 67% (17%) that the USD-HKD exchange rate would break out of the upper (lower) bound. Malz (1997) extracts the risk-neutral probability density function of exchange rate expectations using the second derivative of the price of a European call option (or put option) with respect to its strike price. Genberg and Hui (2011) applies this methodology to study HKD. The dashed red line shows the estimated continuation probability of the peg in our sample, which is higher than the estimates based on the Black-Scholes model. However, it is still substantially

lower than our estimates. In contrast, our model offers more realistic estimates, implying an average probability of 3% of breaking out of either bound. These results illustrate the importance of incorporating possible regime shifts in our framework, compared with the benchmark Black-Scholes model (see, e.g., Genberg and Hui, 2011).

Figure 9: **Peg Survival Probability**



NOTE: This figure plots our estimated probability that the USD-HKD exchange rate will remain within the band based on our model (solid blue lines) and the method in Malz (1997) (dashed red lines), and the standard Black-Scholes model (dotted black lines).

4.2.2 Alternatives to the LERS?

If the LERS were to be abandoned, what could be alternative exchange rate regimes to replace the LERS? In the market commentary, several alternatives have been proposed besides the free float: (1) a link to another currency, say, CNY or CNH; (2) a link to a basket of currencies. In this subsection, we use our estimates of the fundamental value V to assess which alternative is considered to be more realistic by financial market participants.

Table 4 presents regression results examining the relationship between some key economic variables and two estimated measures: the fundamental exchange rate value (V) and the probability of the HKD peg continuing (p). Panel A focuses on V, showing that a decrease in Hong Kong's interbank liquidity (LIQ.) is significantly associated with a lower fundamental value of the HKD. This suggests that liquidity constraints in the financial system exert downward pressure on the HKD's fundamental value. Additionally, the regression reveals

Table 4: Regression Results

	(1)	(2)	(3)	(4)	(5)	(6)
A. V						
LIQ.	-0.01^{***}					-0.01^{**}
	(0.00)					(0.00)
MB		-0.02				0.01
		(0.01)				(0.02)
CNY			0.13^{***}			0.14^{***}
			(0.04)			(0.04)
CNH				0.14^{***}		
				(0.04)		
CFETS					-0.0	0.05
					(0.04)	(0.04)
adj. $R^2(\%)$	3.5	0.6	4.7	6.2	-0.0	7.2
Obs.	203	203	203	160	203	203
B. p						
LIQ.	$0.08***$					$0.11***$
	(0.02)					(0.02)
MB		0.08				$-0.48***$
		(0.15)				(0.17)
CNY			$-1.07***$			$-1.09***$
			(0.40)			(0.41)
CNH				$-0.83***$		
				(0.31)		
CFETS					0.11	-0.36
					(0.36)	(0.37)
adj. $R^2(\%)$	8.4	-0.4	2.9	3.7	-0.5	12.8
Obs.	203	203	203	160	203	203

NOTE: This table reports results from regressions of monthly changes in the fundamental value (i.e., $\Delta log(V_t)$) in Panel A and from those of monthly changes in the continuation probability (i.e., $\Delta log(p_t)$) in Panel B. Columns (1)-(5) report the results from univariate regressions using monthly changes in inter-bank liquidity, monetary base, the spot exchange rates of USD versus CNY and CNH, as well as the CFETS index, respectively. Column (6) reports the results from the regression that uses all the previous regressors at the same time, except the USD-CNH exchange rate to avoid collinearity. The sample period is between January 2007 and December 2023 (and between August 2010 and December 2023 for the regressions using the USD-CNH exchange rate). Monthly observations represent the average of daily data for each month. Significance levels: * $p < .10$; ** $p < .05$; and *** $p < .01$.

a strong positive correlation between V and the CNY and CNH exchange rates, with the coefficients of the latter variables being 0.13 and 0.14, respectively. This indicates that financial markets perceive the HKD's fundamental value as closely linked to the Chinese

currency, suggesting that in the event of a peg break, the HKD might move toward the value of the yuan as an alternative to a free float.

Panel B analyzes the factors influencing the probability, p, that the HKD peg remains intact. Liquidity has a strong positive relationship with p, with the coefficients rangin from 0.08 to 0.11, indicating that higher liquidity supports peg stability. Meanwhile, the monetary base (MB) has a mixed effect. This suggests that an excessive monetary base expansion might weaken confidence in the peg. Additionally, the CNY and CNH exchange rates exhibit strong negative correlations with p, suggesting that as the yuan depreciates, market participants perceive a higher risk of the HKD peg breaking.

Overall, the regression results highlight the HKD's sensitivity to both local liquidity conditions and broader developments in China's currency markets. They reinforce the view that external pressures—particularly those from U.S. monetary policy and China's financial stability—play a crucial role in shaping market expectations about the peg's future.

5 Conclusion

This paper provides an analysis of the sustainability of the HKD-USD peg, a cornerstone of Hong Kong's financial stability for nearly four decades. By developing an asset-pricing model and estimating it using HKD options data, we measure financial markets' views about the likelihood of the peg's persistence. Our findings highlight the significant pressures the peg has faced in recent years, driven by aggressive U.S. interest rate hikes, a widening interest rate differential, and Hong Kong's slower post-pandemic economic recovery.

Our estimates suggest that the perceived probability of the peg breaking surged to approximately 50% in late 2022, a level not seen since the global financial crisis. Additionally, the HKD consistently trading near the weak end of its band and the sharp decline in aggregate liquidity reflect the ongoing depreciation pressure.

While some market participants express skepticism about the peg's sustainability, others, including officials and analysts, remain confident in the HKMA's ability to maintain it. By leveraging both the model and empirical data, this study fills a critical gap in the literature by providing a quantifiable assessment of market perceptions regarding the peg's future. Regular updates to our estimates can serve as an early warning system, enabling regulators and investors to anticipate and respond to changing market conditions.

References

Amador, M., J. Bianchi, L. Bocola, and F. Perri (2019): "Exchange Rate Policies at the Zero Lower Bound," *The Review of Economic Studies*, 87, 1605–1645.

Auer, R., A. Burstein, and S. M. Lein (2021): "Exchange Rates and Prices: Evidence from the 2015 Swiss Franc Appreciation," *American Economic Review*, 111, 652–86.

Ball, C. A. and A. Roma (1993): "A jump diffusion model for the European monetary system," *Journal of International Money and Finance*, 12, 475–492.

Bertola, G. and L. E. O. Svensson (1993): "Stochastic Devaluation Risk and the Empirical Fit of Target-Zone Models," *The Review of Economic Studies*, 60, 689–712.

Bisesti, L., A. Castagna, and F. Mercurio (2005): "Consistent Pricing and Hedging of an FX Options Book," *Kyoto Economic Review*, 74, 65–83.

Blagov, B. and M. Funke (2019): "The regime-dependent evolution of credibility: A fresh look at Hong Kong's linked exchange rate system," *Macroeconomic Dynamics*, 23, 2434–2468.

Breedon, F., L. Chen, A. Ranaldo, and N. Vause (2023): "Judgment day: Algorithmic trading around the Swiss franc cap removal," *Journal of International Economics*, 140, 103713.

Delgado, F. and B. Dumas (1991): "Target zones Big and Small," NBER Working Paper No. 3601.

Dumas, B., L. P. Jennergren, and B. Naslund (1995): "Realignment Risk and Currency Option Pricing in Target Zones," *European Economic Review*, 39, 1523–1544.

Engel, C. (1996): "The forward discount anomaly and the risk premium: A survey of recent evidence," *Journal of Empirical Finance*, 3, 123–192.

Feng, S., L. Fu, C.-Y. Ho, and W.-Y. Alex Ho (2023): "Political stability and credibility of currency board," *Journal of International Money and Finance*, 137, 102911.

Froot, K. A. and M. Obstfeld (1991a): "Exchange-rate dynamics under stochastic regime shifts: A unified approach," *Journal of International Economics*, 31, 203–229.

——— (1991b): "Stochastic Process Switching: Some Simple Solutions," *Econometrica*, 59, 241–250.

Genberg, H. and C.-H. Hui (2011): "The Credibility of Hong Kong's Link from the Perspective of Modern Financial Theory," *Journal of Money, Credit and Banking*, 43, 185–206.

Ghosh, A., A.-M. Gulde, and H. Wolf (2020): "Currency boards," in *Handbook of the History of Money and Currency*, ed. by S. Battilossi, Y. Cassis, and K. Yago, Singapore: Springer, 687–715.

Greenwood, J. (2007): *Hong Kong's Link to the US Dollar: Origins and Evolution*, Hong Kong University Press.

Hanke, M., R. Poulsen, and A. Weissensteiner (2018): "Event-Related Exchange-Rate Forecasts: Combining Information from Betting Quotes and Option Prices," *Journal of Financial and Quantitative Analysis*, 53, 2663–2683.

Hertrich, M. and H. Zimmermann (2017): "On the Credibility of the Euro/Swiss Franc Floor: A Financial Market Perspective," *Journal of Money, Credit and Banking*, 49, 567–578.

Jeanne, O. and P. Masson (2000): "Currency crises, sunspots and Markov-switching regimes," *Journal of International Economics*, 50, 327–350.

Jermann, U. J. (2017): "Financial Markets' Views about the Euro–Swiss Franc Floor," *Journal of Money, Credit and Banking*, 49, 553–565.

Krugman, P. R. (1991): "Target Zones and Exchange Rate Dynamics," *Quarterly Journal of Economics*, 106, 669–682.

Kwan, Y. K. and F. Lui (1999): "Hong Kong's currency board and changing monetary regimes," in *Changes in exchange rates in rapidly developing countries: theory, practice, and policy issues*, University of Chicago Press, 403–436.

Latter, T. (2007): "Rules versus discretion in managing the Hong Kong dollar, 1983-2006," Tech. rep., Hong Kong Institute for Monetary Research.

Lindberg, H. and P. Söderlind (1994): "Intervention Policy and Mean Reversion in Exchange Rate Target Zones: The Swedish Case," *The Scandinavian Journal of Economics*, 96, 499–513.

Lustig, H., N. Roussanov, and A. Verdelhan (2011): "Common Risk Factors in Currency Markets," *Review of Financial Studies*, 24, 3731–3777.

Malz, A. M. (1997): "Estimating the probability distribution of the future exchange rate from option prices," *Journal of Derivatives*, 5, 18–36.

Mirkov, N., I. Pozdeev, and P. Söderlind (2019): "Verbal interventions and exchange rate policies: The case of Swiss franc cap," *Journal of International Money and Finance*, 93, 42–54.

Na, S., S. Schmitt-Grohé, M. Uribe, and V. Yue (2018): "The Twin Ds: Optimal Default and Devaluation," *American Economic Review*, 108, 1773–1819.

Svensson, L. E. (1991a): "Target zones and interest rate variability," *Journal of International Economics*, 31, 27–54.

——— (1991b): "The term structure of interest rate differentials in a target zone: Theory and Swedish data," *Journal of Monetary Economics*, 28, 87–116.

A Proofs

Proof of Proposition 1. Below we use lowercase variables to denote the logarithm of the corresponding uppercase variables. For example, $v_t \equiv \log V_t$, $s^P \equiv \log S^P$, $\widehat{v}_t \equiv \log \widehat{V}_t$, etc.

Similarly, we derive the dynamics of $\widehat{V}_t$ as follows:

$$\frac{d\widehat{V}_t}{\widehat{V}_t} = \frac{dV_t}{V_t} = \mu_V dt + \sigma_V dW_{V,t}. \tag{24}$$

We are now ready to solve the (scaled) equilibrium exchange rate $\widehat{S}(\widehat{V}_t)$. It is straightforward to prove that $\widehat{S}(\widehat{V}_t)$ is monotonically increasing. Define $\widehat{V}_*$ and $\widehat{V}^*$ such that $\widehat{S}(\widehat{V}_*) = 1 - \widehat{b}$ and $\widehat{S}(\widehat{V}^*) = 1 + \widehat{b}$. As the length of the period Δt converges to zero, with probability one $\widehat{V}_{t+\Delta t} > \widehat{V}^*$ (or $\widehat{V}_{t+\Delta t} < \widehat{V}_*$) if $\widehat{V}_t > \widehat{V}^*$ (or $\widehat{V}_t < \widehat{V}_*$). Therefore, from equation (5), it must be true that: $\widehat{S}(\widehat{V}_t) = 1 - \hat{b}$ if $\widehat{V} < \widehat{V}_*$, and $1 + \hat{b}$ if $\widehat{V} > \widehat{V}^*$.

If $\widehat{V} \in (\widehat{V}_*, \widehat{V}^*)$, it is straightforward to show that $\widehat{S}(\widehat{V}_t)$ must satisfy the following equation based on equation (5):

$$\widehat{S}'\left(\widehat{V}_t\right)\widehat{V}_t\mu_V + \frac{1}{2}\widehat{S}''\left(\widehat{V}_t\right)\widehat{V}_t^2\sigma_V^2 + (r_{USD} - r_{HKD} - \lambda)\,\widehat{S}\left(\widehat{V}_t\right) + \lambda\widehat{V}_t = 0. \tag{25}$$

The solution to this ordinary differential equation is: $\widehat{S}(\widehat{V}_t) = C_0\widehat{V} + C_1\widehat{V}^{\eta_1} + C_2\widehat{V}^{\eta_2}$, where η_1 and η_2 are the two roots of the quadratic equation:

$$\frac{1}{2}\sigma_V^2\eta^2 + \left(\mu_V - \frac{1}{2}\sigma_V^2\right)\eta + (r_{USD} - r_{HKD} - \lambda) = 0, \tag{26}$$

and the coefficient C_0 is given by

$$C_0 = \frac{\lambda}{\lambda + r_{HKD} - r_{USD} - \mu_V}, \tag{27}$$

and the coefficients C_1, C_2 and the thresholds $\widehat{V}_*$, $\widehat{V}^*$ are determined from the value-matching and smooth-pasting conditions:

$$\begin{aligned}
\widehat{V}_* + C_1(\widehat{V}_*)^{\eta_1} + C_2(\widehat{V}_*)^{\eta_2} &= 1 - \widehat{b}, & (28)\\
\widehat{V}^* + C_1(\widehat{V}^*)^{\eta_1} + C_2(\widehat{V}^*)^{\eta_2} &= 1 + \widehat{b}, & (29)\\
C_0 + \eta_1 C_1(\widehat{V}_*)^{\eta_1 - 1} + \eta_2 C_2(\widehat{V}_*)^{\eta_2 - 1} &= 0, & (30)\\
C_0 + \eta_1 C_1(\widehat{V}^*)^{\eta_1 - 1} + \eta_2 C_2(\widehat{V}^*)^{\eta_2 - 1} &= 0. & (31)
\end{aligned}$$

■

Proof of Proposition 2. Because $S_t^P \equiv S^P\,(=7.8)$ is a constant, $\widehat{V}_t$ follows the same process in equation (6), implying the following expression for $\widehat{V}_{t+\tau}$

$$\widehat{V}_{t+\tau} = \widehat{V}_t \exp\left\{\left(\mu_V - \frac{1}{2}\sigma_V^2\right)\tau + \sigma_V\sqrt{\tau}z_V\right\},$$

where z_V denotes a random variable with a standard normal distribution. Therefore, $\widehat{V}_{t+\tau} \leq \widehat{V}^*$ if and only if $z_V \leq -d^*$ and $\widehat{V}_{t+\tau} \geq \widehat{V}_*$ if and only if $z_V \geq -d_*$, where the expressions of d^* and d_* are given in equations (10) and (11). Therefore, $H\left(\widetilde{S}_{t+\tau}; S^P, b\right)$ equals $S^P + b$ with probability $1 - \Phi\left(-d^*\right) = \Phi\left(d^*\right)$; $S^P - b$ with probability $\Phi\left(-d_*\right)$; and $S^P\left(C_0\widehat{V}_{t+\tau} + C_1\widehat{V}_{t+\tau}^{\eta_1} + C_2\widehat{V}_{t+\tau}^{\eta_2}\right)$ with probability $\Phi\left(-d^*\right) - \Phi\left(-d_*\right)$.

Second, the date-t conditional expectation of $\widehat{V}_{t+\tau}^{\eta}$ conditional on $\widehat{V}_* \leq \widehat{V}_{t+\tau} \leq \widehat{V}^*$ is given below

$$\begin{aligned}
& E_t^Q\left[\widehat{V}_{t+\tau}^{\eta}\middle|\, \widehat{V}_* \leq \widehat{V}_{t+\tau} \leq \widehat{V}^*\right] \\
= & \frac{\widehat{V}_t^{\eta} e^{\eta\left(\mu_V - \frac{1}{2}\sigma_V^2\right)\tau}}{\Phi\left(-d^*\right) - \Phi\left(-d_*\right)} \int_{-d_*}^{-d^*} \frac{1}{\sqrt{2\pi}} e^{\eta\sigma_V\sqrt{\tau}z_V - \frac{1}{2}z_V^2} dz_V \\
= & \widehat{V}_t^{\eta} e^{\eta\mu_V\tau + \frac{1}{2}\eta(\eta-1)\sigma_V^2\tau} \frac{\Phi\left(-d^* - \eta\sigma_V\sqrt{\tau}\right) - \Phi\left(-d_* - \eta\sigma_V\sqrt{\tau}\right)}{\Phi\left(-d^*\right) - \Phi\left(-d_*\right)} \\
\equiv & \Gamma\left(\widehat{V}_t; \eta\right).
\end{aligned}$$

Substituting the above results into $E_t^Q\left[H\left(\widetilde{S}_{t+\tau}; S^P, b\right)\right]$ yields the expression for $F_S\left(\tau\right)$ in equation (14) where we denote $\eta_0 = 1$. ■

Proof of Proposition 3. (i) Note that

$$\begin{aligned}
C_V\left(K,\tau\right) \equiv & e^{-\widetilde{r}_{HKD}\tau} E^Q\left[\max\left(V_{t+\tau} - K, 0\right)\right] \\
= & e^{-\widetilde{r}_{HKD}\tau} \int_{-d_{2,V}}^{\infty} \left[V_t \exp\left\{\left(\mu_V - \sigma_V^2/2\right)\tau + \sigma_V\sqrt{\tau}z_V\right\} - K\right] \phi\left(z_V\right) dz_V \\
= & e^{-\widetilde{r}_{HKD}\tau} V_t e^{\left(\mu_V - \sigma_V^2/2\right)\tau} \int_{-d_{2,V}}^{\infty} e^{\sigma_V\sqrt{\tau}z_V} \phi\left(z_V\right) dz_V - e^{-\widetilde{r}_{HKD}\tau} K\Phi\left(d_{2,V}\right) \\
= & V_t e^{\left(\mu_V - \widetilde{r}_{HKD}\right)\tau}\left(1 - \Phi\left(-d_{2,V} - \sigma_V\sqrt{\tau}\right)\right) - e^{-\widetilde{r}_{HKD}\tau} K\Phi\left(d_{2,V}\right) \\
= & V_t e^{-r_{USD}\tau}\Phi\left(d_{1,V}\right) - e^{-\widetilde{r}_{HKD}\tau} K\Phi\left(d_{2,V}\right),
\end{aligned}$$

where

(ii) There are three possibilities.

(a) If $K \geq S^P + b$, then $H\left(\widetilde{S}_{t+\tau}; S^P, b\right) \leq S^P + b \leq K$, implying $C_S(K,\tau) = 0$.

(b) If $K \leq S^P - b$, then $H\left(\widetilde{S}_{t+\tau}; S^P, b\right) \geq S^P + b \geq K$, implying $C_S(K,\tau) = e^{-r_{HKD}\tau} E^Q\left[H\left(\widetilde{S}_{t+\tau}; S^P, b\right) - K\right] = e^{-r_{HKD}\tau}\left(F_S(\tau) - K\right)$, where $F_S(\tau)$ is given in equation (14).

(c) If $S^P - b < K < S^P + b$, then there exists a cutoff value, denoted by $\widehat{V}_K \in \left(\widehat{V}_*, \widehat{V}^*\right)$, such that $\widehat{S}(\widehat{V}_K) = \frac{K}{S^P} \equiv \widehat{K}$. Consider three cases. In the first case where $\widehat{V}_{t+\tau} \geq \widehat{V}^*$, we have $H\left(\widetilde{S}_{t+\tau}; S^P, b\right) = S^P + b > K$, implying that the present value of the expected option payoff is $e^{-r_{HKD}\tau}\left(S^P + b - K\right)$. In the second case where $\widehat{V}_{t+\tau} \leq \widehat{V}_*$, we have $H\left(\widetilde{S}_{t+\tau}; S^P, b\right) = S^P - b < K$, implying that the present value of the expected option payoff is zero. In the third case where $\widehat{V}_* \leq \widehat{V}_{t+\tau} \leq \widehat{V}^*$, in this case $H\left(\widetilde{S}_{t+\tau}; S^P, b\right) \geq K$ is equivalent to $\widehat{V}_{t+\tau} \geq \widehat{V}_K$, or equivalently $z_V \geq -d_K$, where the expression of d_K is given in equation (22). Therefore,

$$
\begin{aligned}
& e^{-r_{HKD}\tau} E^Q\left[\max\left(H\left(\widetilde{S}_{t+\tau}; S^P, b\right) - K, 0\right) \middle| \widehat{V}_* \leq \widehat{V}_{t+\tau} \leq \widehat{V}^*\right] \\
= & \frac{e^{-r_{HKD}\tau}}{\Phi(-d^*) - \Phi(-d_*)} \int_{-d_K}^{-d^*} \left(\widetilde{S}_{t+\tau} - K\right) \frac{1}{\sqrt{2\pi}} \exp\left(-\frac{z_V^2}{2}\right) dz_V \\
= & \frac{e^{-r_{HKD}\tau} S^P}{\Phi(-d^*) - \Phi(-d_*)} \int_{-d_K}^{-d^*} \left[C_0 \widehat{V}_{t+\tau} + C_1 \widehat{V}_{t+\tau}^{\eta_1} + C_2 \widehat{V}_{t+\tau}^{\eta_2} - \widehat{K}\right] \frac{1}{\sqrt{2\pi}} \exp\left(-\frac{z_V^2}{2}\right) dz_V \\
= & e^{-r_{HKD}\tau}\left[S^P \sum\nolimits_{i=0}^{2} C_i \Gamma^*\left(\widehat{V}_t; \eta_i\right) - K\Gamma^*\left(\widehat{V}_t; 0\right)\right],
\end{aligned}
$$

where in deriving the second-to-last equality we have used the following result

$$
\begin{aligned}
& \frac{1}{\Phi(-d^*) - \Phi(-d_*)} \int_{-d_K}^{-d^*} \widehat{V}_{t+\tau}^{\eta} \frac{1}{\sqrt{2\pi}} \exp\left(-\frac{z_V^2}{2}\right) dz_V \\
= & \frac{\widehat{V}_t^{\eta} e^{\eta\left(\mu_V - \frac{1}{2}\sigma_V^2\right)\tau}}{\Phi(-d^*) - \Phi(-d_*)} \int_{-d_K}^{-d^*} \frac{1}{\sqrt{2\pi}} e^{\eta\sigma_V\sqrt{\tau}z_V - \frac{1}{2}z_V^2} dz_V \\
= & \widehat{V}_t^{\eta} e^{\eta\mu_V\tau + \frac{1}{2}\left(\eta^2 - \eta\right)\sigma_V^2\tau} \frac{\Phi\left(-d^* - \eta\sigma_V\sqrt{\tau}\right) - \Phi\left(-d_K - \eta\sigma_V\sqrt{\tau}\right)}{\Phi(-d^*) - \Phi(-d_*)} \\
\equiv & \Gamma^*\left(\widehat{V}_t; \eta\right).
\end{aligned}
$$

Therefore, in summary, the option price is given below when $S^P - b < K < S^P + b$,

$$
\begin{aligned}
& C_S(K,\tau) \\
= & \left(1 - \Phi(-d^*)\right) e^{-r_{HKD}\tau}\left[S^P + b - K\right] \\
& + \left(\Phi(-d^*) - \Phi(-d_*)\right) e^{-r_{HKD}\tau}\left[S^P \sum\nolimits_{i=0}^{2} C_i \Gamma^*\left(\widehat{V}_t; \eta_i\right) - K\Gamma^*\left(\widehat{V}_t; 0\right)\right].
\end{aligned}
$$

The derivation for put options is similar. For example,

$$\begin{aligned}
& e^{-r_{HKD}\tau} E^Q \left[\max\left(K - H\left(\widetilde{S}_{t+\tau}; S^P, b \right), 0 \right) \middle| \widehat{V}_* \leq \widehat{V}_{t+\tau} \leq \widehat{V}^* \right] \\
= & \frac{e^{-r_{HKD}\tau}}{\Phi(-d^*) - \Phi(-d_*)} \int_{-d_*}^{-d_K} \left(K - \widetilde{S}_{t+\tau} \right) \frac{1}{\sqrt{2\pi}} \exp\left(-\frac{z_V^2}{2} \right) dz_V \\
= & \frac{e^{-r_{HKD}\tau} S^P}{\Phi(-d^*) - \Phi(-d_*)} \int_{-d_*}^{-d_K} \left[\widehat{K} - \left(C_0 \widehat{V}_{t+\tau} + C_1 \widehat{V}_{t+\tau}^{\eta_1} + C_2 \widehat{V}_{t+\tau}^{\eta_2} \right) \right] \frac{1}{\sqrt{2\pi}} \exp\left(-\frac{z_V^2}{2} \right) dz_V \\
= & e^{-r_{HKD}\tau} \left[K\Gamma_*\left(\widehat{V}_t; 0 \right) - S^P \sum\nolimits_{i=0}^{2} C_i \Gamma_*\left(\widehat{V}_t; \eta_i \right) \right],
\end{aligned}$$

where

$$\begin{aligned}
& \frac{1}{\Phi(-d^*) - \Phi(-d_*)} \int_{-d_*}^{-d_K} \widehat{V}_{t+\tau}^{\eta} \frac{1}{\sqrt{2\pi}} \exp\left(-\frac{z_V^2}{2} \right) dz_V \\
= & \frac{\widehat{V}_t^{\eta} e^{\eta\left(\mu_V - \frac{1}{2}\sigma_V^2\right)\tau}}{\Phi(-d^*) - \Phi(-d_*)} \int_{-d_*}^{-d_K} \frac{1}{\sqrt{2\pi}} e^{\eta\sigma_V\sqrt{\tau} z_V - \frac{1}{2} z_V^2} dz_V \\
= & \widehat{V}_t^{\eta} e^{\eta\mu_V\tau + \frac{1}{2}\left(\eta^2 - \eta\right)\sigma_V^2\tau} \frac{\Phi\left(-d_K - \eta\sigma_V\sqrt{\tau}\right) - \Phi\left(-d_* - \eta\sigma_V\sqrt{\tau}\right)}{\Phi(-d^*) - \Phi(-d_*)} \\
\equiv & \Gamma_*\left(\widehat{V}_t; \eta \right).
\end{aligned}$$

■